ORNL/TM-2021/2122

Measuring Hydroxylammonium, Nitrate, and Nitrite Concentration with Raman Spectroscopy for the ^{238}Pu Supply Program

Travis J. Hager
Luke R. Sadergaski

August 2021

OAK RIDGE National Laboratory

ORNL IS MANAGED BY UT-BATTELLE LLC FOR THE US DEPARTMENT OF ENERGY

ORNL/TM-2021/2122

Radioisotope Science and Technology Division

MEASURING HYDROXYLAMMONIUM, NITRATE, AND NITRITE WITH RAMAN SPECTROSCOPY FOR THE ^{238}PU SUPPLY PROGRAM

Travis J. Hager
Luke R. Sadergaski

August 2021

Prepared by
OAK RIDGE NATIONAL LABORATORY
Oak Ridge, TN 37831-6283
managed by
UT-BATTELLE, LLC
for the
US DEPARTMENT OF ENERGY
under contract DE-AC05-00OR22725

CONTENTS

LIST OF FIGURES

LIST OF TABLES

ABBREVIATIONS

LOD	determine limit of detection
LOQ	limit of quantification
ORNL	Oak Ridge National Laboratory
REDC	Radiochemical Engineering Development Center
SNV	standard normal variate

ACKNOWLEDGMENTS

Funding for this program was provided by NASA's Science Mission Directorate and administered by the US Department of Energy, Office of Nuclear Energy, under contract DEAC05-00OR22725. This work used resources at the High Flux Isotope Reactor, a Department of Energy Office of Science User Facility operated by Oak Ridge National Laboratory. This work was supported in part by the U.S. Department of Energy, Office of Science, Office of Workforce Development for Teachers and Scientists (WDTS) under the Science Undergraduate Laboratory Internship Program.

EXECUTIVE SUMMARY

Optical spectroscopy has great potential to improve the timeliness of important analytical measurements for the ^{238}Pu Supply Program by enabling real-time analysis of process solutions within radiochemical hot cells. Hydroxylammonium (H_3NOH^+]), nitrate (NO_3^-), and nitrite (NO_2^-) are three important molecular species present in multiple aqueous streams throughout the program's flow sheet. The concentration of each species normally goes uncharacterized during processing. However, rapid quantification may benefit the program because uncertainties in kinetic redox expressions describing hydroxylammonium (HA) and nitrite reactions with Np and Pu leads to uncertainty in process model predictions for solvent extraction runs. HA concentration is normally quantified using ion chromatography, a technique that requires diluted grab samples taken out of the hot cell and analyzed off-line. Here we evaluate Raman spectroscopy for determining the concentration of H_3NOH^+, NO_3^-, and NO_2^- in benchtop tests to determine limits of detection. We also consider the possibility of using Raman spectroscopy in both glove box and hot cell environments for rapid analysis and pinpoint additional development opportunities needed to make this application successful.

ABSTRACT

Hydroxylammonium (HA^+) is a reductant used during selective Pu solvent extraction for the ^{238}Pu Supply Program. Optical spectroscopic techniques can be used for nondestructive quantification of molecular species within shielded hot cells. Analytes of interest in this work are HA^+, nitrate, and nitrite. Raman spectroscopy is proposed as a simple method for direct real-time quantification of these species. The vibrational modes of each compound were identified, and the best mode was used to determine limit of detection (LOD) and limit of quantification (LOQ). For HA^+, the strongest band was attributed to the N–OH symmetric ν_5 vibrational mode at 1,007 cm^{-1}. With our setup, the LOD and LOQ for HA^+ ranged from 0.0018 to 0.0037 mol/L and from 0.0059 to 0.011 mol/L, respectively. Nearly a factor two difference in detection limit was attributed to the application of different preprocessing methods before the analysis. These results suggest that detection limits useful for monitoring the process can be achieved using Raman spectroscopy. Future development may include incorporating Raman self-absorption effects that will be encountered in solutions containing Pu and optimizing data processing selection methods.

1. BACKGROUND AND MOTIVATION

1.1 BACKGROUND

The ^{238}Pu Supply Program at Oak Ridge National Laboratory (ORNL) produces ^{238}Pu for NASA. This highly radioactive alpha-emitter is used as a heat source for thermoelectric generators.[1] Neptunium-237, contained in mixed aluminum–NpO_2 cermet pellets, undergoes transmutation during irradiation at the High Flux Isotope Reactor via neutron capture and subsequent beta decay of neptunium-238 to plutonium-238. After irradiation, targets are dissolved in nitric acid, and the Pu is extracted and purified via a variety of radiochemical separations. The first separation in the flow sheet is selective Pu liquid–liquid extraction.[2] A key part of this process is the reduction of Pu(IV) to Pu(III) using hydroxylammonium (HA^+) nitrate. Common reductants in an analogous step for PUREX applications are U(IV) nitrate, Fe(II) sulfamate, and hydroxylammonium nitrate (HAN).[3] Thus, measuring HA^+ concentration is important for ^{238}Pu Supply Program and other nuclear fuel cycle applications.

HA^+ is a highly reactive species that undergoes several autocatalytic reactions to produce many gaseous products, so it needs to be handled carefully. Despite this, it is a favorable because of the downsides of other reductants. Uranium(IV) nitrate needs to be stabilized with hydrazine and will introduce unwanted uranium in the chemical system. Iron(II) sulfamate is highly corrosive to stainless steel and causes the waste to become difficult to manage.[3] HAN is formed by the ionic pairing of a protonated hydroxylamine group with a nitrate ion. This complex forms from hydroxylamine conjugate acid (i.e., hydroxylammonium [HA^+]) in aqueous nitric acid solutions commonly used for Pu extractions. There are two predominant irreversible reactions that describe Pu(IV) reduction to Pu(III) using HA^+:

$$2NH_3OH^+ + 2Pu^{4+} \rightarrow 2Pu^{3+} + N_2O_{(g)} + H_2O + 6H^+ \quad (1)$$

$$2NH_3OH^+ + 2Pu^{+4} \rightarrow 2Pu^{3+} + N_{2(g)} + 2H_2O + 4H^+ \quad (2)$$

HA^+ can decompose by reacting with nitrite generated by alpha radiolysis, which is a significant reaction that the ^{238}Pu program must consider because of the strong alpha emitter ^{238}Pu.[4] Nitrites not only decompose HA^+, but they can also reoxidize Pu(III).[4] Additionally, nitrites in solution form nitrous acid, which reacts with HA^+ by the following reactions:[5]

$$NH_3OH^+ + HONO \rightarrow N_2O + H_2O + H_3O^+ \quad (3)$$

$$NH_3OH^+ + 2HONO_2 + 2HONO \rightarrow 5HONO + H_3O^+ \quad (4)$$

Monitoring the concentration of HA^+ during and after processing is important because mishandling has led to runaway reactions that resulted in physical harm.[6] HA^+ concentration measurements would ideally take place within hot cells to improve the timeliness and simplicity of these time-sensitive analytical measurements. Achieving real-time analysis with optical spectroscopy in a hot cell environment is challenging.[7] Online spectroscopic methods can be verified by robust chemical analyses with low detection limits applied in adjacent glove boxes and radiochemical hot cells.

1.2 RAMAN SPECTROSCOPY

Vibrational Raman spectroscopy is a molecular spectroscopic technique appealing for chemical analysis because it is a nondestructive technique based on optical phenomena, and it can be applied to solids, liquids, or gases with minimal sample preparation. A sample is irradiated by monochromatic light, and some of the incident radiation is scattered by molecular bond vibrations. For a bond to be Raman active, vibrations induced by the photon must cause a change in the polarizability.[8] There are three types of Raman scattering: Rayleigh, Stokes, and anti-Stokes. Rayleigh scattering is an elastic collision where the scattered light has the same energy as the induced light but changes direction. Stokes scattering is the inelastic scattering of light that results in a photon of lower energy than the incident light equivalent to one vibrational transition. Anti-Stokes scattering is inelastic scattering of light that results in a photon of higher energy than the incident light also corresponding to a vibrational transition. Stokes scattering is more intense than anti-Stokes scattering because of the population of vibrational energy levels. The vibrational modes are characteristic of the molecular structure.[8] Unlike infrared spectroscopy that is based on vibrational absorption rather than scattering, Raman is useful for aqueous systems as the different selection rules mean that Raman scattering of H_2O is weak.

Raman spectroscopy is notable for its simplicity. Instrumental requirements include a monochromatic light source (laser), sample holder (solid, liquid, or gas), fiber optics, and a perpendicular detection system to the incident light source or Raman probe. This simplicity makes it an appealing method for chemical analysis in hot cell online monitoring applications. In situ measurements are possible when using optical fibers, which can transmit light hundreds of meters.[1] Raman scattered light is directly proportional to the concentration of the scattering molecule in the sample.[9] This property enables the quantification of analyte concentration based on Raman signal intensity.

With a perfect analytical instrument, all the information obtained through the chemical analysis would come from the system being monitored and no other source. This is impossible to achieve, but there are methods to reduce the amount of noise present in data. In Raman spectroscopy, noise can be classified into five groups: photon shot noise, sample-generated noise, instrument-generated noise, computationally generated noise, and externally generated noise.[9] The most common source is sample-generated noise. An important limitation of Raman spectroscopy is the prominence of other optical processes. This includes phenomena, such as, absorbance, fluorescence, and the presence of blackbody radiation from hot samples. Sometimes, Raman scattered light can coincide with the absorbance cross section of another component of the chemical system. Absorbance processes generally have larger cross sections and thus greater intensity. This self-absorbance phenomenon can make quantitative Raman analysis more challenging. To counteract this, collecting Raman spectra in reflection mode with a minimal focal distance improves Raman signal intensity.

1.3 MOTIVATION

Before considering hot cell applications, detection limits for HA^+, nitrate, and nitrite concentration must be determined using the Raman spectrometer. If the desired detection limits are achieved, this approach

could provide several operational benefits including rapid, in situ, and user-friendly analysis compared with off-line methods such as ion chromatography. This more common method for quantifying HA^+ concentration requires significant dilutions because of the high nitrate concentration and transfer of the samples out of the hot cell for analysis. This could be circumvented by the direct analysis using Raman spectroscopy. Raman analysis could also provide detailed kinetic expressions for HA^+ redox reaction(s) with Np and Pu in controlled glove box studies. These data could be incorporated into solvent extraction models to predict concentration profiles of Np and Pu, which is a need described in our previous work.[1]

2. MATERIALS AND METHODS

2.1 MATERIALS

Chemicals were commercially obtained (ACS grade). Concentrated nitric acid (70%) and hydroxylammonium nitrate (24 wt%) were purchased from Sigma-Aldrich. Samples were prepared using deionized water with a resistivity of 18.2 MΩ·cm at 25 °C.

2.2 CALIBRATION AND VALIDATION STANDARDS

Solutions containing hydroxyl ammonium nitrate (0–0.5 M) and sodium nitrite (0–0.5 M) were prepared using volumetric glassware. Each solution was pipetted into 1.8 mL borosilicate glass vials (VWR Scientific, 66009-882) for Raman analysis.

2.3 RAMAN SPECTROSCOPY AND DATA ANALYSIS

A Horiba iHR-320 spectrometer was used to collect stokes Raman spectra with a 532 nm laser source (Cobalt Samba 150) operating at 90 mW. Static measurements were recorded in triplicate from 500 to 3,850 cm^{-1} using a 1,200 grooves/mm grating with a resolution of 0.9 cm^{-1}. A general-purpose Raman probe made by Spectra Solutions Inc. was used to collect Raman spectra in reflection mode with an 8 second integration time. The probe had a 9 mm focal length and a 7 mm working distance and was placed in a probe and sample cuvette holder made by Spectra Solutions Inc. (see Figure 2.1). The Unscrambler X (version 10.4) software was used for data preprocessing, which included standard normal variate analysis and a first derivative. Preprocessing operations were selected based on user experience and will be discussed later. A linear fit analysis was calculated using OriginPro software to determine the error in the intercept for determining detection limits.

Figure 2.1. General-purpose Raman probe and sample holder made by Spectra Solutions Inc.

3. RESULTS AND DISCUSSION

3.1 RAMAN SPECTRA

3.1.1 Raman spectrum of hydroxylammonium nitrate

The hydroxyl ammonium cation NH_3OH^+ (HA^+) has an identity operation and only one plane of symmetry, which places it in the C_s symmetry group. The conjugate base, NH_2OH is also described by the C_s point group. Based on molecular symmetry calculations, 12 distinct vibrational bands (8 symmetric and 4 antisymmetric) were identified for each molecule. Each mode is Raman active and summarized in Table 3.1. In our work, three vibrational bands for HA^+ were clearly identified including the strong ν_5 at 1,007 cm^{-1}, a very weak ν_8 peak at 1,239 cm^{-1}, and a broad ν_4 shoulder at 1,552 cm^{-1}.

Table 3.1. Vibrational modes.

NH_3OH^+			NH_2OH		
Frequency (cm^{-1})	**No.**	**Assignment[10]**	**Frequency (cm^{-1})**	**No.**	**Assignment[11]**
1,004	ν_5	N–O stretching	407	ν_9	O–H torsion
1,168	ν_6, ν_6'	NH_3 rocking	955	ν_6	N–O stretch
1,204	ν_8, ν_8'	O–H plane bending	1,192	ν_5	NH_2-wag
1,496	ν_3	NH_3 sym. deformation	1,347	ν_8	NH_2-twist
1,565	ν_4, ν_4'	NH_3 asym. deformation	1,429	ν_4	NOH-bend
2,926	ν_1	N–H_3 sym. stretching	1,703	ν_3	HNH-bend
2,970	ν_7	O–H stretching	3,531	ν_7	NH asym. stretch
3,000	ν_2	N–H_3 asym. stretching	3,636	ν_2	NH sym. stretch
3,050	ν_2'	N–H_3 asym. stretching	3,892	ν_1	OH-stretch

The peak corresponding to the N–O symmetric stretching band of HA^+ was identified at 1,007 cm^{-1} (see Figure 3.1). Hydroxylamine was not identified because of the lack of a Raman peak at 955 cm^{-1}. Other peaks corresponding to nitrate and the water band are also labeled in Figure 3.1.

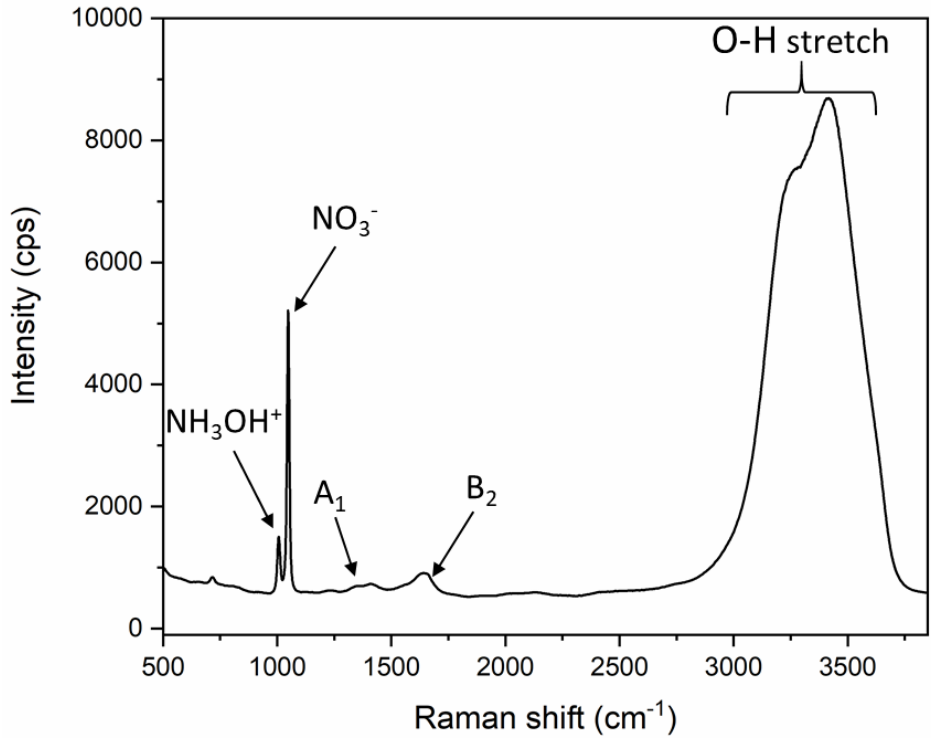

Figure 3.1. Raman spectrum of a solution comprised of 0.5 M HAN in water. The most intense peaks are labeled and correspond to the NH_3OH^+ symmetric N–O stretch at 1,007 cm^{-1}, the NO_3^- symmetric N–O stretch at 1,048 cm^{-1}, and the water band O–H stretching region from ~2,800 to 3,800 cm^{-1}. The weak A1 and B2 pair associated with ν_3 antisymmetric band are also labeled.

The allowed vibrational modes and resulting spectral fingerprint of the protonated and deprotonated forms of hydroxylamine are unique. Acid/base chemistry was considered to determine the species present in solution. The dissociation hydroxylammonium nitrate and the acid/base equilibrium expressions for (NH_3OH^+) are shown in equations 5–7. In acidic solutions, hydroxylamine will normally adopt its conjugate acid form (i.e., NH_3OH^+).

$$NH_3OHNO_3(l) \rightarrow NH_3OH^+(aq) + NO_3^-(aq) \quad (5)$$

$$NH_3OH^+ + H_2O \rightleftharpoons NH_2OH + H_3O^+ \quad (6)$$

$$k_a = \frac{[NH_2OH][H^+]}{NH_3OH^+} \quad (7)$$

As HA^+ is a weak acid, it does not contribute a significant concentration of free acid (H^+) to the system. Based on its acid dissociation constant (pKa) value of 6.03, the free acid concentration in a 0.1 M HAN solution is 4.3×10^{-4} M (pH 3.36). Thus, the predominant species in solution is HA^+, which is corroborated by the selection rule assessment and the Raman spectra. In these applications, nitric acid will be present in solutions containing HAN, and the pH will be far below the pKa of HA^+. Thus, the analysis herein describes the appropriate species.

Free nitrate ions possess D_{3h} symmetry and are described by four possible vibrational bands. They are A_1' ν_1 symmetric N–O stretching, A_2'' ν_2 out of plane bending, E' ν_3 antisymmetric stretching, and E' ν_4 in-plane bending.[12] Of these four vibrational bands, only ν_1, ν_3, and ν_4 are Raman active. However, NO_3^- undergoes symmetry deformations in polar solvents and in the presence of cations (e.g., HA^+).[13] This

reduces the symmetry of nitrate from D_{3h} to C_{2v} and thus splits the degenerate ν_3 and ν_4 into A_1 and B_2 pairs. With C_{2v} symmetry, only ν_3 shows symmetry of its A_1 and B_2 pair with an observed splitting. The ν_4 split modes include a Raman active B_2 symmetry mode and a silent A_1 mode.[13] This explains why only five nitrate peaks were observed in this data. The band at 715 cm^{-1} is associated to the ν_4 in-plane bending with E' symmetry under D_{3h}. The primary band at 1,048 cm^{-1} is assigned to the ν_1 symmetric N–O stretching. The A_1 and B_2 pair associated to the splitting of the ν_3 antisymmetric stretching band is found at 1,340 and 1,660 cm^{-1} (see Figure 3.1). The B_2 mode overlaps with a water O–H bending mode at ~1640 cm-1.

3.1.2 Raman of nitrite

The nitrite ion has the same point group as water, C_{2v}. This means that it has three allowed vibrational modes, and each one is Raman active. These include the symmetric (A_1) ν_1 N–O stretching mode and ν_2 N–O bending modes and an asymmetric (B_2) ν_3 N–O stretching mode with peak positions at 813, 1240, and 1,331 cm^{-1}, respectively.[14] We observe the ν_1 peak at 815 cm^{-1}, the ν_2 peak at 1,234 cm^{-1}, and the ν_3 peak at 1,332 cm^{-1} (see Figure 3.2). The least sensitive ν_2 peak appears as a weak shoulder next to the most intense ν_3 peak.

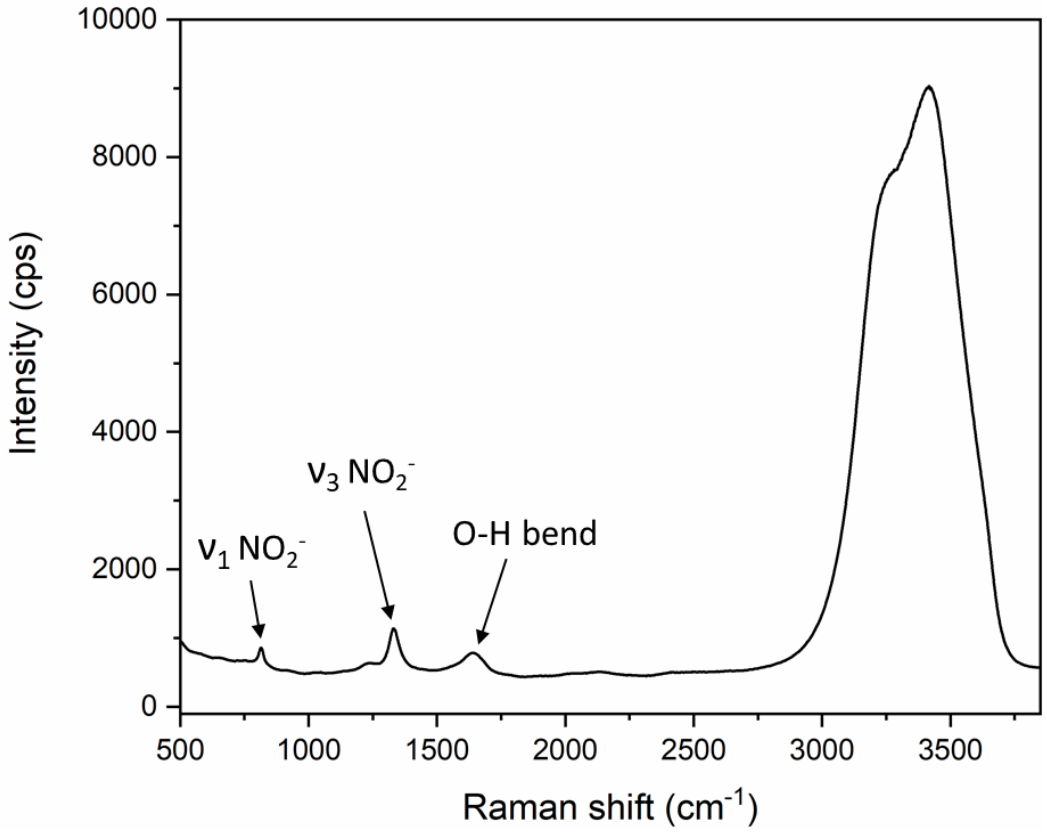

Figure 3.2. Raman spectrum of 0.5 M $NaNO_2$. The most intense peak is labeled and corresponds to the NO_2^- N–O asymmetric stretch at 1,332 cm^{-1}. Additional peaks are labeled and correspond NO_2^- symmetric ν_1 peak at 815 cm^{-1} and the H_2O ν_2 O–H bending peak at 1,643 cm^{-1}.

3.1.3 Raman water band

Water molecules, with a C_{2v} symmetry, have three Raman active vibrational modes. The polarized ν_1 O–H stretching (3,280 cm^{-1}) and the ν_2 O–H bending (1,643 cm^{-1}) modes are totally symmetric (A_1), whereas

the ν_3 O–H antisymmetric stretch (3,408 cm^{-1}) is depolarized. Hydrogen bonding causes the O–H stretching vibrations to shift in frequency, resulting in inhomogeneous broadening.[15] This is due in part to electron delocalization across hydrogen bonds, which increase the O–H bond length.[16] The water band can be deconvoluted into five Gaussian peaks based on the assumption of various water clusters.[15] The overlapping peaks are not analyzed in this study but were clearly observed in the Raman spectra (see Figures 3.1 and 3.2). This region of the spectrum will be used in future work focused on multivariate data analysis to determine nitric acid concentration. This methodology can even be used to determine solution temperature by analyzing the O–H stretching region.[17]

4. LIMIT OF DETECTION AND LIMIT OF QUANTIFICATION

Two data preprocessing methods were tested to remove scatter effects and baseline offsets before quantitative analysis. A standard normal variate (SNV) transformation removes multiplicative scatter effects by centering and scaling spectra. First derivatives remove baseline offsets in the spectra. The most characteristic features of a first derivative spectrum are the point it passes through zero (at the maximum peak position) and the positive and negative bands on either side of this point. These correspond to the inflection points in the original peak and appeared at 1,001/1,013 cm^{-1} and 1,043/1,053 cm^{-1} for the HA^+ and nitrate peaks, respectively (see Figure 3.3). The 1,001 and 1,053 cm^{-1} peaks for HA^+ and nitrate were chosen for the linear regression because they did not overlap. The same preprocessing steps were applied to Raman spectra collected on sodium nitrate solutions (0.05–0.5 M) before analysis. The resulting positive and negative peak positions from the inflections points of the most intense 1,332 cm^{-1} nitrite peak appeared at 1,316 and 1,345 cm^{-1}. In addition to SNV, a first derivative with a 3rd order polynomial and a 13-point smoothing window was applied to the data. For comparison, data were also preprocessed using only a first derivative with a third order polynomial and a 25-point smoothing window.

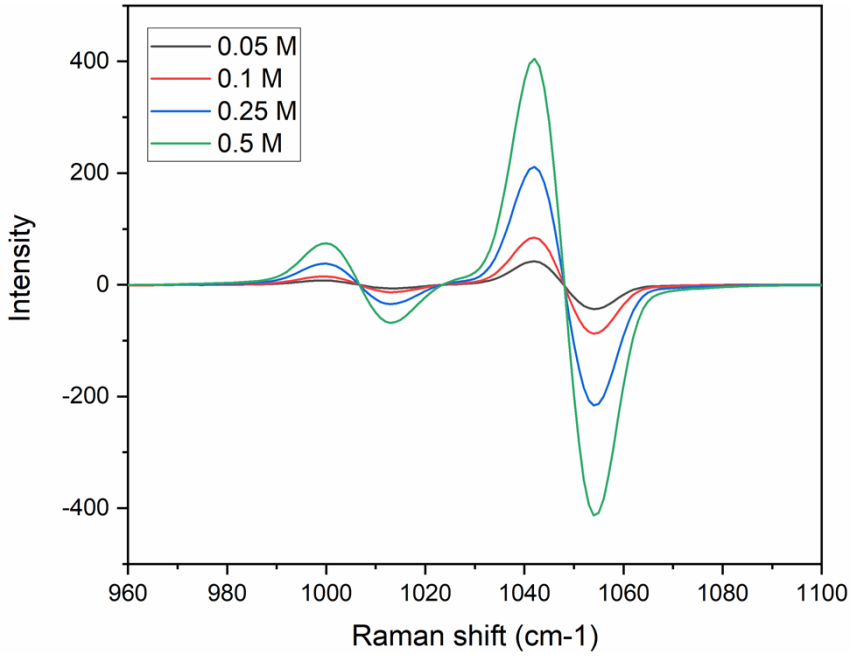

Figure 4.1. First derivative Raman spectra of solutions containing 0.05–0.5 M HAN. Data in this figure were preprocessed using the SNV transformation, third order polynomial, and a first derivative with a 13-point smoothing window.

Univariate linear regressions describing the relationship between concentration and the most prominent Raman band peak intensity were used to determine the detection limit of each species. The linear

regression model was in $y = mx + b$ form, where y describes the Raman intensity values and x represents concentration values. Example for HA^+ and nitrate are shown in Figure 4.2. The standard deviation of the intercept of each linear regression was calculated using OriginPro software and used to determine the limit of detection and limit of quantification of the spectra by the equations 1 and 2, where σ_b is the standard deviation of the y-intercept calculated using a 95% confidence interval.

$$LOD = \frac{3\sigma_b}{m} \quad (1)$$

$$LOQ = \frac{10\sigma_b}{m} \quad (2)$$

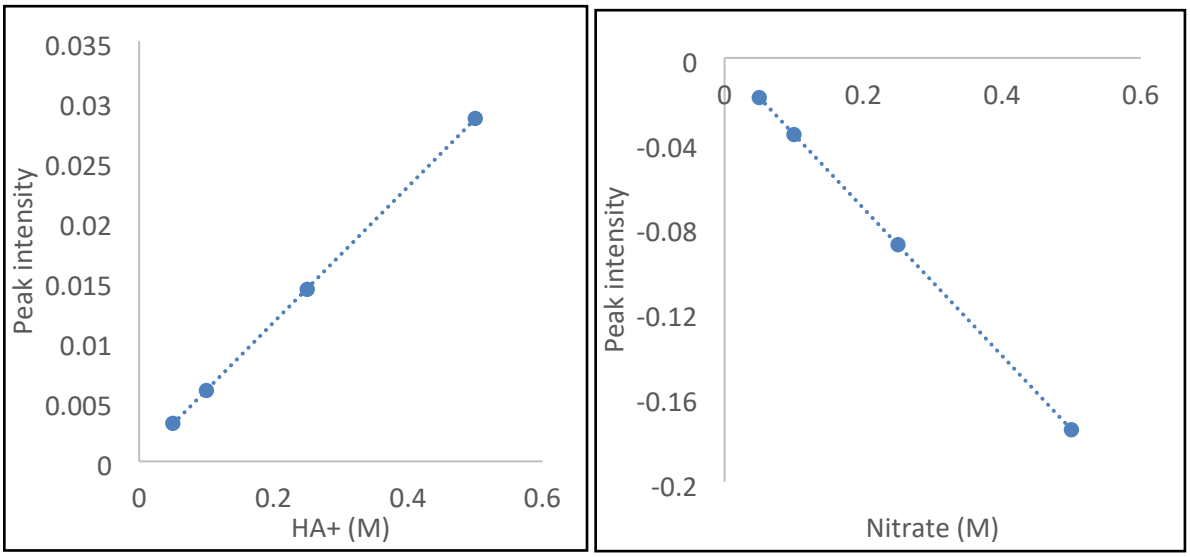

Figure 4.2. Linear regression of the hydroxylammonium ion (HA^+) (*left*) and nitrate (*right*) peak intensities vs. concentration.

Hydroxylammonium LOD and LOQ were calculated using the 1,001 cm^{-1} peak in the derivative spectra. The nitrate LOD and LOQ were calculated using the negative 1,053 cm^{-1} peak. However, the nitrite LOD and LOQ were calculated using both the positive 805 and negative 1,333 cm^{-1} peaks for comparison. The negative nitrite derivative peak at 1,344 cm^{-1} was chosen because it did not overlap with the shoulder corresponding to the ν_2 peak at 1,233 cm^{-1}.

LOD and LOQ values for each analysis (HA^+, nitrate, and nitrite) are shown in Tables 4.1–4.3. The detection limits for HA^+ and nitrate changed significantly based on the preprocessing method. This finding highlights the need to develop a robust and efficient preprocessing selection method, which will be addressed in a separate research publication. The best limits of detection for nitrite were calculated using the positive inflection point (at 805 cm^{-1}) of the symmetric nitrite peak centered near 817 cm^{-1}. It performed better than the negative inflection peak corresponding to the asymmetric stretch, even though that peak was more intense in the original Raman spectrum (see Figure 3.2). This finding makes the nitrite analysis in the presence of HAN more straightforward because neither HA^+ nor nitrate have confounding vibrational modes at this position.

Table 4.1. LOD and LOQ values with SNV and 1st derivative preprocessing.

Analyte	LOD (M)	LOQ (M)
Hydroxylammonium	0.0037	0.011
Nitrate	0.0010	0.0034
Nitrite	0.013	0.043

Table 4.2. LOD and LOQ values with only first derivative preprocessing.

Analyte	LOD (M)	LOQ (M)
Hydroxylammonium	0.0018	0.0059
Nitrate	0.0073	0.011
Nitrite	0.017	0.055

These LOD and LOQ values were achieved using an excitation energy of 90 mW. Although our laser can operate at 180 mW, we chose to operate at a lower energy to emulate the power loss that we might expect taking Raman measurements in a glove box. Raman signal intensity is directly proportional to excitation energy so if the same acquisition parameters were used, and the power was increased to 180 mW, the LOD and LOQ values would be expected to improve by roughly a factor of two. Fluorescent background signals are not expected to be an issue at higher laser power. A new 532 nm laser operating at <500 mW could also be acquired if enhanced detection limits are desired. A laser power of 500 mW and above transitions from a class 3b to a class 4 laser, and additional safety measures would be required.

5. SUMMARY AND MAJOR CONCLUSIONS

5.1 FUTURE STUDIES AND APPLICATIONS

In the future, self-absorption due to the presence of Pu in solutions is something that will need to be considered. The absorption spectra of Pu(III) and Pu(IV) overlap with the excitation frequency (532 nm) and the Raman spectrum of HAN. Although another laser excitation frequency could be selected, it likely would not make a difference because Pu(III/IV) absorbs light over the entire visible–near infrared region (400–1,100 nm) and Raman analysis outside of this region is not feasible. It is unlikely that the nitrate peak will be distorted or shift peak position because the acidity used in most relevant applications (i.e., low acid ≤ ~1 M nitric) does not allow the formation of Pu(IV) nitrato complexes. However, the overall intensity may decrease due to self-absorption effects. The Raman probe working distance (i.e., position of focal optics) could be minimized to maximize the signal. This may be accounted for with a re-optimized combination of preprocessing transformations (e.g., multiplicative scatter corrections).

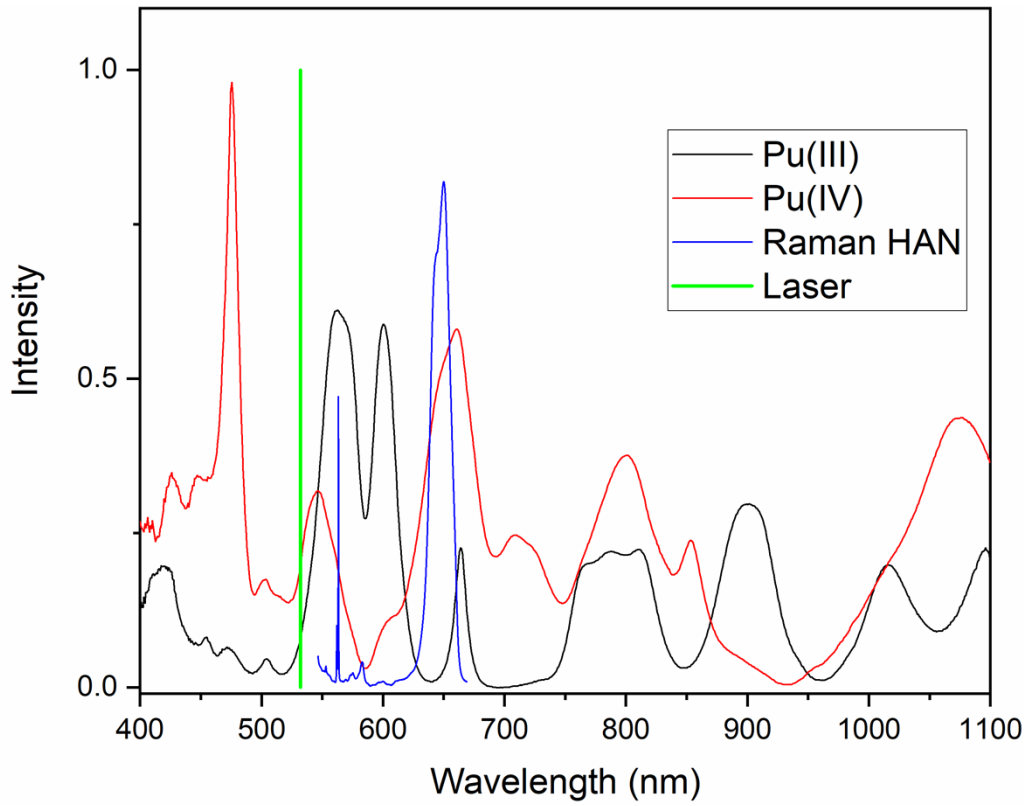

Figure 5.1. Plutonium(III) (7 g Pu(III)/L) and Pu(IV) absorption spectrum compared to a scaled Raman spectrum of 0.5 M HAN and the excitation wavelength (532 nm). Raman shift (cm^{-1}) units were converted to wavelength (nm).

This work demonstrated that Raman spectroscopy can achieve useful quantification limits for HA^+ and nitrate and useful detection limits for nitrite as well. With the appropriate online monitoring software (e.g., Process Pulse II by Camo Analytics), Raman spectroscopy could be used for the near real-time monitoring of HAN concentration for the ^{238}Pu Supply Program. Because of the multicomponent nature of Raman spectra, many reports have demonstrated the use of multivariate regression analysis for species quantification.[17,18] Future work will include multivariate data analysis and compare prediction performance of partial least squares regression models to the detection limits achieved in this report. Another aspect to investigate further is the optimization of the method for determining preprocessing methods using optimal experimental design.

Although the desired limit of quantification level for nitrite was not achieved in this study (i.e., 0.01 mol/L), there is another comparable option that could improve sensitivity. UV-resonance Raman spectroscopy is a method that increases the intensity of Raman scattering by the inclusion of UV-resonance absorption. All molecules have molecular electronic absorption band frequencies that can be excited with specific excitation energies. Some Raman scattering electron cloud oscillations are near the same frequency as these absorption bands and have great coupling. This increases the induced dipole moment of a molecule, which increases the probability of scattering.[19,20] This increases the intensity of Raman scattering by 10^8 in some cases compared to normal Raman measurements.[18] Detection limits of <14 µM could be achieved with an excitation energy of 204 and 229 nm for nitrite and nitrate.[20] A third harmonic of a Coherent Inc. Infinity Nd:YAG laser in H_2 and a Coherent Inc. CW intracavity frequency-doubled argon ion laser could be used to obtain a 204 and 229 nm excitation source respectively. UV excitation is highly selective and tends to avoid fluorescence interferences from other species in solution.

Another interesting study could investigate UV resonance Raman spectroscopy for enhanced detection limits for HA^+.

CONCLUSIONS

This work demonstrated that Raman spectroscopy is a viable method of the quantification of hydroxylammonium, nitrate, and nitrite. Molecular symmetry calculations allow for the identification of Raman active vibrational bands that correspond to NH_3OH^+. The univariate approach outlined here is applicable in solutions that do not contain Np or Pu. Future work will focus on a multivariate approach for HA^+ and free acid quantification, how to efficiently select an optimal combination of preprocessing transformations and determine the extent of self-absorption effects in systems containing Pu.

REFERENCES

[1] Sadergaski, L.; Myhre, K.; Delmau, L.; Benker, D.; DePaoli, D.; Wham, R. "Spectroscopic and Multivariate Analysis Development in Support of the Plutonium-238 Supply Program." *Nuclear and Emerging Technologies for Space*, 2020.

[2] Gallmeier, E.; Gallmeier, K.; McFarlane, J.; Morales-Rodriguez, M. "Real Time Monitoring of the Chemistry of Hydroxylamine Nitrate and Iron as Surrogates for Nuclear Materials Processing." 2019, *Separation Science and Technology*, 54:12, 1985–1993.

[3] Paviet-Hartmann, P.; Riddle, C.; Campbell, K.; Mausolf, E. *Overview of Reductants Utilized in Nuclear Fuel Reprocessing/Recycling*. 2013, INL/CON-12-28006 Idaho National Laboratory, Idaho Falls, ID.

[4] McFarlane, J.; Delmau, L.; DePaoli, D.; Mattus, C.; Phelps, C.; Roach, B. *Hydroxylamine Nitrate Decomposition under Non-radiological Conditions.* 2015, ORNL/TM-2015/156. Oak Ridge National Laboratory, Oak Ridge, TN.

[5] Raman, S.; Ashcraft, R.; Vial, M.; Klasky, M. "Oxidation of Hydroxylamine by Nitrous and Nitric Acids. Model Development from First Principle SCRF Calculation." *J. Phys. Chem.*, 2005. 109(38), 8526–8536

[6] Durant, W.; Gray, L.; Wallace, R.; Yau, W. *Explosions and Other Uncontrolled Chemical Reactions at Non-Reactor Nuclear Facilities of the Savannah River Plant*. 1988, DP-MS-88-15. Argonne National Laboratory, Lemont, IL.

[7] Morales-Rodriguez, M.; McFarlane, J.; Kidder, M. "Quantum Cascade Laser Infrared Spectroscopy for Online Monitoring of Hydroxylamine Nitrate." *International Journal of Analytical Chemistry*, 2018.

[8] Atkins, P.; De Paula, J.; Keeler, J. *Physical Chemistry* 11th ed. 2018: Oxford University Press.

[9] Pelletier, M. "Quantitative Analysis Using Raman Spectrometry." *Appl. Spectrosc.* 2003. 57, 20A–42A.

[10] Krishnan, R.; Balasubramanian, K. "Raman Spectrum of Hydroxylamine Hydrochloride ($NH_3OH.Cl$)." *Proc. Indian Acad. Sci.* 1964. 59, 285–291.

[11] Luckhaus, D. "The Rovibrational Dynamics of Hydroxylamine." *Ber. Bunsenges. Phys. Chem.* 1997. **101**(3), 346–355.

[12] Klein, N.; Wong, K. N. *An Infrared Investigation of HAN-based Liquid Propellants.* 1987, AD-A187 226. US Army Ballistic Research Laboratory, Aberdeen, MD.

[13] Waterland, M.; Stockwell, D.; Kelly, A. "Symmetry Breaking Effects in NO_3^-: Raman Spectra of Nitrate Salts and ab initio Resonance Raman Spectra of Nitrate-water Complexes." *J. Chem. Phys.* 2001, 114, 6249.

[14] Sidman, J. "Electronic and Vibrational States of the Nitrite Ion. II. Vibrational States." *J. Am. Chem. Soc.* 1957, 79(11), 2675–2678

[15] Sun, Q. "Logical Statistical Interpretation for Water Structure." *Chemical Physics Letters.* 2013 568, 90–94.

[16] Ludwig, R. "The Effect of Hydrogen Bonding on the Thermodynamic and Spectroscopic Properties of Molecular Clusters and Liquids." *Phys. Chem. Chem. Phys.*, 2002, 4, 5481–5487

[17] Casella, A.; Levitskaia, T.; Peterson, J.; Bryan, S. "Water O–H Stretching Raman Signature for Strong Acid Monitoring via Multivariate Analysis." *Anal. Chem.* 2013, 85, 4120–4128.

[18] Sadergaski, L. R. DePaoli, D. W.; Myhre, K. G. "Monitoring the Caustic Dissolution of Aluminum Alloy in a Radiochemical Hot Cell Using Raman Spectroscopy." *Appl. Spectrosc.* 2020, 74(10), 1252–1262.

[19] Kudelski, A. "Analytical Applications of Raman Spectroscopy." *Talanta*. 2008, 76, 1-8

[20] Asher, S. "UV Resonance Raman Spectroscopy for Analytical, Physical, and Biophysical Chemistry." *Am. Chem. Soc.* 1993, 2(65), 59A–65A